Pol. J. Environ. Stud. Vol. 27, No. 6 (2018), 2765-2774
DOI: *10.15244/pjoes/81063* ONLINE PUBLICATION DATE: 2018-06-25

Original Research

Effective Removal of Humic Acid Using Strontium-Doped TiO_2 Coated on Porous Ceramic Filter Media in Water Resource

Trinh Xuan Tung[1, 2, 3], Dong Xu[2]*, Yi Zhang[2], Qiaohong Zhou[2], Zhenbin Wu[1, 2]**

[1]School of Resources and Environmental Engineering, Wuhan University of Technology, Wuhan, P.R. China
[2]State Key Laboratory of Freshwater Ecology and Biotechnology, Institute of Hydrobiology, Chinese Academy of Sciences, Wuhan, P.R. China
[3]Vietnam Maritime University, Haiphong, Vietnam

Received: 10 October 2017
Accepted: 7 December 2017

Abstract

A photocatalyst comprised of strontium-doped TiO_2 coated on porous ceramic filter media (Sr-TiO_2/PCFM) was prepared using the heat-treated process. The main objective of this study was to investigate the effects of catalyst dosage, initial HA concentrations, pH, and temperature on the adsorption and degradation of humic acid (HA) in a solution containing Sr-TiO_2/PCFM under irradiation of UV light. Removal efficiency of 84.25% for HA was achieved under experimental conditions for a Sr-TiO_2/PCFM dosage of 80 g at an initial concentration of 15 mg/L over a period of 8 h. Higher degradation was found for HA in the acidic environment and at higher operating temperatures. The rate of the adsorption reaction followed the pseudo second-order kinetics with the sorption isotherm well fitted to the Freundlich and Langmuir isotherm models. The oxidation rate constants of HA were evaluated by using pseudo first-order kinetics that can describe the photodegradation process. Furthermore, the photocatalytic stability of Sr-TiO_2/PCFM was performed with 3 cycles reused. These findings suggest that the Sr-TiO_2/PCFM was found to be an effective and promising approach to eliminating HA in water resources.

Keywords: adsorption, photocatalytic, humic acid (HA), strontium-doped TiO_2 coated on porous ceramic filter media (Sr-TiO_2/PCFM), water resource

Introduction

Humic substances are among the most important natural organic matters (NOM) existing in ground and surface waters and are known as one of the main disinfection by-product (DBPs) precursors that may act as health risk factors [1]. Humic substances – mainly humic acids (HA), which constitute the major fraction of NOM in water supplies – have been suggested as a standard for mimicking NOM in the laboratory. HA are non-biodegradable and have color, odor, and also exhibit a wide range of distribution in molecular weight and

*e-mail: xudong@ihb.ac.cn
**e-mail: wuzb@ihb.ac.cn

size [2]. HA includes both hydrophobic and hydrophilic components as well as many chemical functions that can provide many available sites for the binding of metal ions and thereby greatly affect the growth of plants and microorganisms [3]. Meanwhile, HA could bind with organic chemicals that may influence the toxicity of these compounds to plants and microorganisms [4]. During the disinfection of municipal drinking water treatments, HA can react with chlorine, resulting in the formation of trihalomethanes that cause cancer and seriously affect human health [5]. Owing to the harmful effects noted above, HA removal from water is necessary and has been attempted in different ways.

The degradation of HA can proceed through a variety of methods such as coagulation, precipitation, filtration, ion-exchange, use of activated carbon, or biological treatment. However, the application of the proposed methods is associated with a number of disadvantages. For example, the coagulation process brings some disadvantages but coagulation and flocculation followed by sedimentation/flotation and filtration have been considered as the most common and economically feasible process for removing HA. Within 45 min by coagulation, approximately 81% of HA was removed, but Al^{3+} residual might bring some risks for drinking water [6]. Taking into account the disadvantages of these methods, the heterogeneous photocatalytic degradation processes involving titanium dioxide (TiO_2) can be regarded as an effective alternative solution for eliminating HA from water resources [7-9].

Although TiO_2 exists in 3 polymorphs (anatase, rutile, and brookite), only the first two have value in photocatalysis [10]. When illuminated with light of wavelength ≤380 nm, the TiO_2 particle (anatase form) produces excited-state electrons and hole pairs (e^-_{CB}/h^+_{VB}) where the pre-adsorbed O_2 and H_2O molecules react. That can migrate to the surface to form a powerful oxidizing agent (e.g., $HOO^{\bullet}$, hydroxyl radicals $OH^{\bullet}$, and superoxides $O_2^{\bullet-}$). These radical species possess the potential to oxidize various organic molecules. Due to its high adsorption ability to organic contaminants corresponding with good quality photocatalytic efficiency, TiO_2 photocatalysts have been used in many types of reactor configurations, including circulating columns, fluidized beds, membrane reactors, and immobilized films [11]. By using many different techniques, TiO_2 can be immobilized on ceramic, glass, plastic, and polyvinyl chloride-coated fabrics [12-13]. To facilitate the practical application of the photocatalytic process, the finding out of a suitable carrier substrate for synthesizing and immobilizing crystalline TiO_2 is required. The porous ceramic filter media (PCFM) possesses a high surface area with large porosity, high adsorption capacity, and suitable pore structure used in the paper as carrier material of the TiO_2 thin film.

The aim of this work was to evaluate the adsorption characteristics and photocatalytic activities of strontium-doped TiO_2 coated on porous ceramic filter media (Sr-TiO_2/PCFM) for the removal of HA from a water resource under various experimental conditions. The adsorption kinetics and isotherm for the removal of HA by Sr-TiO_2/PCFM were evaluated. The effects of experimental parameters such as the Sr-TiO_2/PCFM dosage, initial HA concentration, pH, and temperature were studied to investigate the feasibility of applying Sr-TiO_2/PCFM for photocatalytic degradation of HA. The stability of the catalyst was also investigated through repeated use of Sr-TiO_2/PCFM.

Materials and Methods

Preparing Sr-TiO_2/PCFM

Due to being composed of small nanocrystallites of rutile being dispersed within an anatase matrix and "quantum size" effect, TiO_2 P25 (Degussa) powder type added with a certain amount of strontium chloride ($SrCl_2$) was chosen for better photocatalytic activity. TiO_2 powder and $SrCl_2$ were mixed in a weight ratio of 50:1, respectively. 100 mL sodium metasilicate solution 20 g/L (Na_2SiO_3) was added and then stirred at 150 rpm until that mixture became thick and dry. The PCFM preprocessed with diluted hydrochloric acid (HCl) 1:9 was rinsed several times with distilled water until a neutral pH was reached and then dried in the oven. Following this, 100 g dried PCFM was slowly added to 100 mL of the above mixture solution for stabilizing. The prepared photocatalyst was mixed, dried at 100ºC for 1 h, and then carefully calcined. The temperature was slowly increased (2ºC/min) to 500ºC and maintained at this level for 3 h. Finally, the heat-treated sample was labeled as Sr-TiO_2/PCFM.

Materials and Analytical Methods

All the chemicals and reagents used in this study were used without further purification. All glassware and sample bottles were soaked in diluted HCl solution for 12 h, then washed and rinsed 3 times with deionized water obtained from the Millipore UV apparatus. Deionized water was also used for the preparation of solutions. All experiments were conducted in duplicate and the average values were used for data analysis.

In this study, the PCFM was provided by Shandong Aluminium Industry Corporation in China. Table 1

Table 1. Chemical compositions of the porous ceramic filter media (wt %).

Compositions	SiO_2	Al_2O_3	Fe_2O_3	CaO	Na_2O	MgO	K_2O
Content	38.25	21.96	18.07	8.64	9.14	2.90	0.52

shows the chemical compositions of ceramic filter media (and does not take into account a few alkali metals and alkaline-earth metals oxides). The PCFM consists primarily of SiO_2 (38.25%), Al_2O_3 (21.96%), and Fe_2O_3 (18.07%).

The surface morphology of the Sr-TiO_2/PCFM was characterized by using JSM-5610LV scanning electron microscopy (SEM) at an accelerating voltage of 20.0 kV. The crystalline phase of Sr-TiO_2/PCFM was identified by x-ray diffraction (XRD, D / MAX-RB RU-200B) operating at 12 kW over the 2θ range 3-145°. The average crystal size of Sr-TiO_2/PCFM was calculated using the Debye-Scherrer equation:

$$D = \frac{0.9\lambda}{\beta(2\theta)cos\theta} \quad (1)$$

…where D is mean crystallite size (nm), λ is the wavelength of the x-ray radiation (λ = 0.1540 nm), β is full-width at half-maximum (FWHM) of the (101) plane (in radians), and θ is the Bragg angle [14].

The humic acid sodium salt was supplied by Alfa Aesar (Shanghai, China). Before mixing the HA solution with the adsorbent, its pH values were adjusted using sodium hydroxide (NaOH 0.1 M) or hydrochloric acid (HCl 0.1 M). The pH of HA solution was measured by using the ST2100 model pH meter (Changzhou, China). The concentration of HA was determined by a UV-vis spectrophotometer (Shimadzu UV-1800 model) at the wavelength 254 nm (UV_{254}).

Adsorption Experiments

The HA stock solution was prepared by dissolving a certain amount of HA into the double-distilled water and then stirred at 600 rpm for 24 h in the dark to improve solution stability. For removing the insoluble matter, a 0.45 μm through membrane filter was used. The stock solution was stored at 5ºC in a refrigerator in the dark. Such a prepared HA solution was stable for weeks.

To evaluate adsorption characteristics of HA on the Sr-TiO_2/PCFM material, adsorption kinetics were performed in dark conditions varying the initial concentration of HA. The stock solution was diluted with an appropriate amount of distilled water to obtain the desired concentration a range of 15-65 mg/L. Adsorption equilibrium experiments were performed by adding respectively 80 g Sr-TiO_2/PCFM with 100 mL of different initial concentrations of HA solutions unadjusted pH at room temperature (25±2ºC) and kept in dark conditions for 8 h. All batch experiments were covered by aluminum foil throughout the experimental period to minimize light impacts on test parameters. At the end of the 1 h interval, 2 ml of HA solution sample was removed, centrifuged, and analyzed for the contaminant concentration. UV_{254} was measured in 10 mm quartz cells in a double-beam spectrophotometer, as the concentration of HA in solution changes. The percent of HA removal was calculated using the following equation:

$$Removal\ (\%) = \frac{(C_o - C_e)}{C_o} x100\% \quad (2)$$

…where C_0 and C_e are the initial and final remaining concentrations of HA (mg/L), respectively. The amount of HA adsorbed by Sr-TiO_2/PCFM material q_e (mg/g) at equilibrium was calculated by Eq. (3):

$$q_e(mg/g) = (C_o - C_e)\frac{V}{m} \quad (3)$$

…where V is the volume of the HA solution (L) and m is the mass of Sr-TiO_2/PCFM used (g).

Photocatalytic Degradation Experiments

All the experiments were operated under laboratory conditions and performed in duplicate. The experimental procedure involved placing a 250 mL glass cup of filtered solution. A high-pressure mercury lamp (125 W, λ_{max} = 365 nm, 40 mW/cm^2) provided an intense light source and was located at the top of the reactor. The degradation efficiency (%) of HA was calculated by Eq. (4), where C_e and C_t are the equilibrium concentration of HA after adsorption and the remaining concentration of HA at a certain time t, respectively:

$$Degradation\ efficiency\ (\%) = \frac{(C_e - C_t)}{C_e} x100\% \quad (4)$$

Before the photocatalytic experiment, the mixing of Sr-TiO_2/PCFM and HA solution sample was put in the dark from 4 to 8 h to reach an adsorption-desorption equilibrium, then the concentration of HA was noted C_e. After irradiation, the investigated solution sample was collected at 1 h intervals and transferred to a vessel of 2 ml volume. Next, transferred samples were centrifuged at the rate of 13,000 rpm for 15 minutes and then analyzed for contaminant concentration. Mineralization of organic carbon was determined by measuring total organic carbon (TOC) value during the photocatalytic degradation of HA.

The stability of the photocatalyst was assessed through repeated use of Sr-TiO_2/PCFM. Repeat experiments were carried out with 15 mg/L HA concentration, an appropriate amount of Sr-TiO_2/PCFM, and 8 h UV irradiation for cycling run. After the first photocatalytic reaction, the remaining solution was replaced with fresh HA solution of 15 mg/L. The used Sr-TiO_2/PCFM is rinsed several times with distilled water for the next cycles. The above procedure was repeated for 3 cycles.

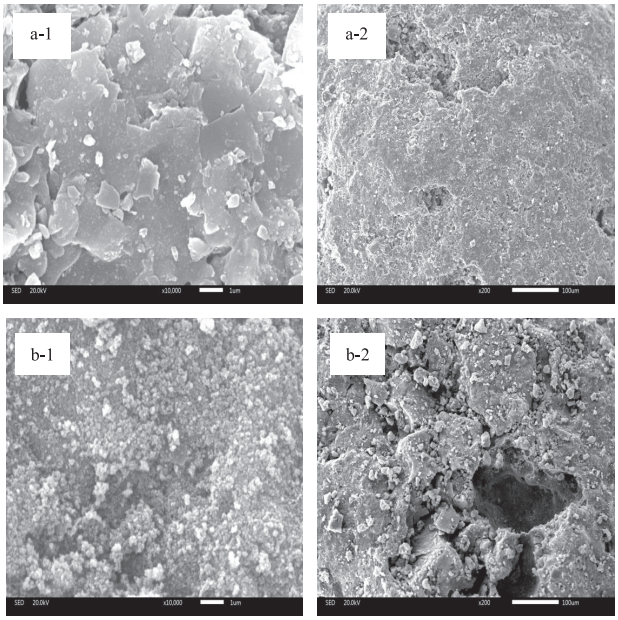

Fig. 1. SEM photograph of (a 1, 2) PCFM and (b 1, 2) Sr/TiO_2-PCFM.

Results and Discussion

Characterization of Sr-TiO_2/PCFM

As shown in Fig. 1(a-1, 2), the surface of the ceramic filter ball is smooth and shows a slice layer. Besides that, its pore structure is enough and distributed uniformly, and provides a good site for TiO_2 particles to be covered. From Fig. 1(b-1, 2), it can be seen that the TiO_2 particles were well dispersed on the surface of PCFM, and some particles embedded in the PCFM under SEM were in the range of the nanometer scale. TiO_2 particles on the external surface will have more chances for Sr-TiO_2/PCFM to receive light and exhibited higher catalytic activity.

For comparison, the crystalline structures of both PCFM and Sr/TiO_2-PCFM were analyzed by XRD pattern and the result is shown in Fig. 2. Their typical diffraction peaks at 2θ = 25.23° corresponded to the (101) planes of anatase, while the peaks at 2θ = 26.54° were in good agreement with the (120) planes of rutile. The result clearly indicated that TiO_2 was successfully loaded onto the ceramic filter and that Sr/TiO_2-PCFM exhibited a mixture of anatase/rutile phases. However, the mean crystallite size of the Sr/TiO_2-PCFM was 39.2 nm – bigger than the P25 TiO_2 that may probably be caused by the incorporation of impurities on the ceramic filter.

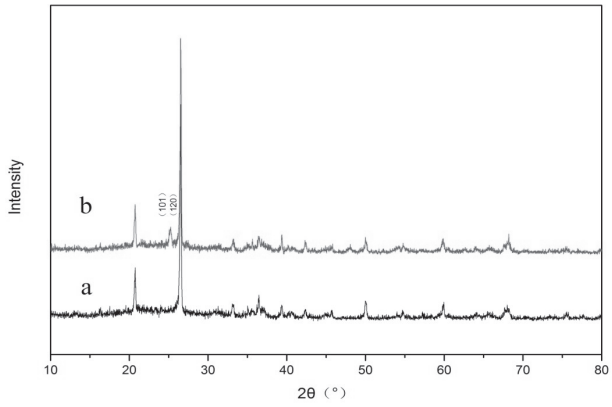

Fig. 2. XRD patterns of a) PCFM and b) Sr/TiO_2-PCFM.

Adsorption Studies

It is noted that the decrease of HA concentration in solution might be caused not only by photodegradation reaction but also by the adsorption of HA on the TiO_2 surface. In order to investigate the effectiveness of the HA removal in a photocatalytic process, the influence of the adsorption of HA from the solution on the Sr-TiO_2/PCFM surface should be determined. It is difficult to predict the adsorption behavior of HA because little is known about its precise molecular structure.

Equilibrium Contact Time

The contact time necessary to reach equilibrium depends on the initial HA concentration [15]. The effect of contact time on the adsorption of HA onto Sr-TiO_2/PCFM at different initial HA concentrations is presented in Fig. 3. It was found that the adsorption of HA on Sr-TiO_2/PCFM occurred and equilibrium adsorption was reached almost in about 4 h with 80 g of Sr-TiO_2/PCFM employed. The amount of adsorbed HA at equilibrium conditions decreased as HA concentration decreased, due to the higher adsorbate concentration, the more diffusion would occur from the adsorbent surface into the micropores [16]. The adsorption capacity at equilibrium increased and the initial rate of adsorption was greater for high initial HA concentrations, while the percentage of adsorption decreased as the initial HA concentration increased from 15 mg/L to 65 mg/L.

Adsorption Isotherms

Some of the most important data in the use of an adsorbent is the adsorption isotherm [16, 17], which

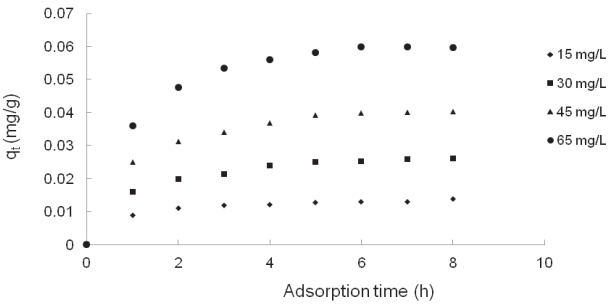

Fig. 3. Equilibrium adsorbed amount of HA onto Sr-TiO_2/PCFM according to adsorption time at various initial HA concentrations.

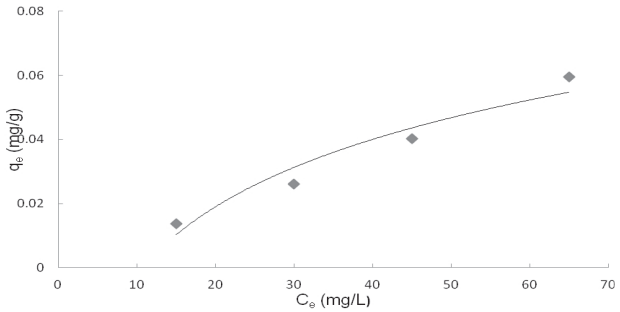

Fig. 4. Adsorption isotherm for HA on the surface of Sr-TiO_2/PCFM.

reflects the relationship between the mass of the solute adsorbed per unit mass of adsorbent and the solute concentration of the solution at equilibrium.

The adsorption isotherm linear HA adsorbed by Sr-TiO_2/PCFM material in this study was shown in Fig. 4 and described by Langmuir and Freundlich isotherms, which were the most commonly employed models. The Freundlich and Langmuir model in their related linearized expressions are expressed by Eqs (5-6), respectively:

$$\frac{1}{q_e} = \frac{1}{q_m K_L C_e} + \frac{1}{q_m} \tag{5}$$

$$logq_e = \frac{1}{n} logC_e + logK_F \tag{6}$$

…where q_e is the equilibrium amount of HA adsorbed per unit weight of the adsorbent (mg/g), C_e is the equilibrium concentration of HA in solution (mg/L), q_m is the maximum adsorption capacity (mg/g), K_L is a constant related to the affinity of the binding sites (L/mg), K_F ((mg/g)(mg/L)$^{-1/n}$), and n indicates the adsorption capacity and a measure of the deviation from linearity of the adsorption, respectively. The Langmuir isotherm constants (K_L) and q_m are obtained from the plot of $1/q_e$ against $1/C_e$ in Eq. (5). The Freundlich constants K_F and $1/n$ are be obtained from the plot of $log(q_e)$ against $log(C_e)$ in Eq. (6). If n is close to 1, the surface heterogeneity could be assumed to be less significant, and as n approaches 10, the impact of surface heterogeneity becomes more significant [18].

Parameter values and correlation coefficients for both isotherms were listed in Table 2. Based on the correlation coefficients (R^2), the experimental results indicated that the sorption of HA onto Sr-TiO_2/PCFM followed both Freundlich and Langmuir models. The constant related to the affinity of the binding sites (K_L) was 0.011 L/mg, and adsorption intensity ($1/n$) was 0.930, implying that the distribution of TiO_2 on the surface of PCFM is even.

To determine if the adsorption process is favorable or unfavorable for the Langmuir-type adsorption process, the Langmuir isotherm is then classified using a dimensionless constant separation factor (R_L), which can be defined as Eq. (7) [19]:

$$R_L = \frac{1}{1+K_L C_o} \tag{7}$$

…where C_0 is the initial concentration of HA (mg/L) at room temperature. If the value of R_L<1, it indicates a favorable adsorption and R_L>1 means unfavorable adsorption [16]. The R_L values for the adsorption of HA onto Sr-TiO_2/PCFM were in the range $0<R_L<1$ (Table 3), indicating that Langmuir adsorption is favorable for the adsorption of HA onto Sr-TiO_2/PCFM.

Adsorption Kinetics

To understand the dynamics of the adsorption reaction regarding the order of the rate constant, the kinetic adsorption data were evaluated. Two kinetic models were applied to investigate the behavior of the adsorption process of HA onto the Sr-TiO_2/PCFM. These models include the pseudo first- and second-order kinetics. The linear forms of reversible pseudo first-order can be formulated as follows:

$$\ln(q_e - q_t) = \ln(q_e) - k_1 t \tag{8}$$

…where q_e (mg/g) and q_t (mg/g) are amounts of HA adsorbed on the Sr-TiO_2/PCFM material at equilibrium and various times, respectively, and k_1 (h^{-1}) is the pseudo first-order rate constant. The values of k_1 were determined from the slope and the intercepts of the plots of $ln(q_e-q_t)$ versus t data.

The linear form of pseudo second-order equation can be formulated as:

$$\frac{t}{q_t} = \frac{1}{k_2 q_e^2} + \frac{t}{q_e} \tag{9}$$

…where k_2 (g/mg.h) is the pseudo second-order rate constant and was determined with q_e from the slope and intercept of the plot of t/q_t versus t. The linear plot of t/q_t as a function of t provides not only the constant rate k_2 but also an independent evaluation of q_e.

Table 2. Adsorption constants for humic acid on the surface of Sr-TiO_2/PCFM.

Langmuir isotherm			Freundlich isotherm		
R^2	K_L (L/mg)	q_m (mg/g)	R^2	K_F ((mg/g)(mg/L)$^{-1/n}$)	1/n
0.991	0.011	3.632	0.983	0.004	0.930

Table 3. Fitted parameters of adsorption isotherm using the consensus of constant separation factor.

HA initial concentration (mg/L)	15	30	45	65
R_L	0.853	0.745	0.660	0.574

The values obtained for k_1 and q_e are presented in Table 4 and Fig. 5. The R^2 values for the pseudo first-order kinetics at different concentrations were relatively low. The calculated q_e values obtained from pseudo first-order kinetics failed to match the experimental q_e values. On the other hand, the correlation coefficients for the pseudo second-order kinetic at different initial HA concentrations were above 0.991 and the calculated $q_{e.cal}$ values were close and agreed well with the experimental data $q_{e.exp}$, particularly at low concentrations. Therefore, it can be said that the adsorption of HA onto Sr-TiO_2/PCFM followed the pseudo second-order reaction model. The equilibrium sorption capacity q_e in this study increased from 0.0139 mg/g to 0.0630 mg/g when the initial concentration of HA increased from 15 mg/L to 65 mg/L. The values of the rate constant were also found to increase from 0.64 x 10^{-5} (g/mg.h) to 55.8 x 10^{-5} (g/mg.h), for an increase in the initial concentration from 15 mg/L to 65 mg/L.

Photocatalytic Degradation of HA by Sr-TiO_2/PCFM

Many studies have discussed the mechanism of photocatalytic oxidation processes between HA with TiO_2 [19-25] and could be expressed by Eq. (10-21).

The simplified mechanism:

$$TiO_2 + hv \rightarrow e_{CB}^- + h_{VB}^+ \quad (10)$$

e_{CB}^- reactions:

$$O_2 + e_{CB}^- \rightarrow O_2^- \quad (11)$$

$$O_2^- + H^+ \rightarrow HO_2^{\cdot} \quad (12)$$

$$HO_2^{\cdot} + HO_2^{\cdot} \rightarrow H_2O_2 + O_2 \quad (13)$$

$$H_2O_2 + e_{CB}^- \rightarrow OH^{\cdot} + OH^- \quad (14)$$

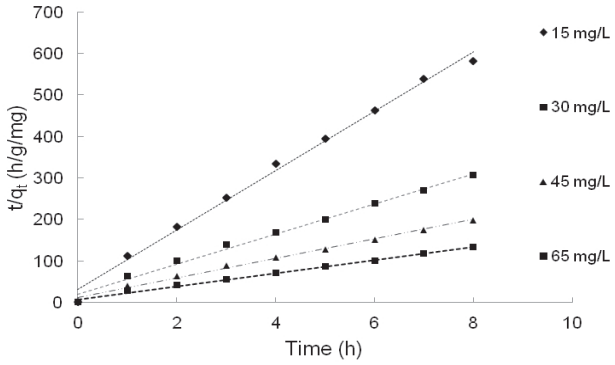

Fig. 5. Pseudo second-order kinetics of HA onto Sr-TiO_2/PCFM.

$$H_2O_2 + O_2^- \rightarrow OH^{\cdot} + OH^- + O_2 \quad (15)$$

$$H_2O_2 + hv \rightarrow 2OH^{\cdot} \quad (16)$$

h_{VB}^+ reactions:

$$h_{VB}^+ + H_2O \rightarrow H^+ + OH^{\cdot} \quad (17)$$

$$OH^- + h_{VB}^+ \rightarrow OH^{\cdot} \quad (18)$$

The redox reactions:

$$HA + OH^{\cdot} \rightarrow H_2O + CO_2 + other\ degradation\ products \quad (19)$$

$$HA + TiO_2(h_{VB}^+) \rightarrow oxidation\ products \quad (20)$$

$$HA + TiO_2(e_{CB}^-) \rightarrow reduction\ products \quad (21)$$

UV illumination on that wavelength for such photon energy usually corresponds to λ<380 nm, and TiO_2 particles on the Sr-TiO_2/PCFM surface or porous structure interact with UV light to generate electron (e_{CB}^-) and hole (h_{VB}^+). The H_2O or O_2 molecules on the surface of TiO_2 particles trap these holes and yield $O_2^{\cdot-}$ and $OH^{\cdot}$ radicals. Generally, $OH^{\cdot}$ radicals, which are the most powerful oxidizing agents, attack the HA molecule through hydroxyl addition or hydrogen extraction effect, and HA converses to CO_2, H_2O, and other degradation products through the different paths. The addition of $OH^{\cdot}$

Table 4. Parameters of adsorption kinetics for HA on Sr-TiO_2/PCFM.

Initial concentration (mg/L)	$q_{e.exp}$ (mg/g)	First-order kinetics			Second-order kinetics		
		k_1	$q_{e.cal}$ (mg/g)	R^2	k_2	$q_{e.cal}$ (mg/g)	R^2
15	0.0138	0.001	1.006	0.600	0.64 x 10^{-5}	0.0139	0.994
30	0.0262	0.002	1.010	0.663	3.84 x 10^{-5}	0.0276	0.991
45	0.0403	0.003	1.017	0.646	15.4 x 10^{-5}	0.0425	0.993
65	0.0594	0.005	1.026	0.626	55.8 x 10^{-5}	0.0630	0.994

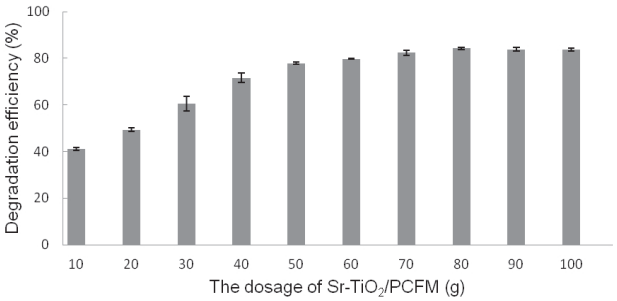

Fig. 6. Effect of Sr-TiO_2/PCFM dosage on the photocatalytic degradation of HA.

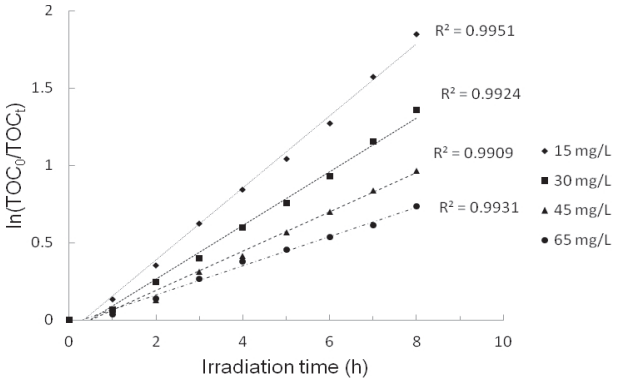

Fig. 7. Pseudo first-order kinetics of the photocatalytic degradation of HA at different initial concentrations.

to aromatic sites in HA leads the result in the formation of ring-opened products, which may contribute to decreases in molecular size, which may later yield CO_2 and H_2O and other degradation products.

In summary, the molecular structures of HA can be broken down or rearranged by the photocatalysis process, which can convert the non-biodegradable organics to more biodegradable forms. Afterward, the photocatalytic activity of Sr-TiO_2/PCFM was evaluated under various experimental conditions: the Sr-TiO_2/PCFM dosage, the initial concentration of HA, the initial pH values, and temperature.

Effect of Sr-TiO_2/PCFM Dosage

The optimum dosage of Sr-TiO_2/PCFM on HA adsorption was carried out for the same initial HA concentration (15 mg/L) at unadjusted pH and different Sr/TiO_2-PCFM dosages. The time of the experiment was 8 h (Fig. 6). From the course of the curve recorded, it has to be concluded that the increase in mineralization degree of HA was enhanced from 41.11% to 77.90% when the dosage of Sr-TiO_2/PCFM was increased from 10 g to 50 g, respectively. The significant differences were also recorded between 50 g and 80 g Sr-TiO_2/PCFM dosages, and maximum HA removal efficiency was 84.25% at dosages beyond 80 g (due to increasing the amount of catalyst dosage contributing to making a large number of active sites available for a fixed concentration of HA). However, no further increase of degradation efficiency value was observed when the Sr-TiO_2/PCFM dosage was increased from 80 g to 100 g. The percentage removal decreased slightly at higher 80 g dosage of the Sr-TiO_2/PCFM. It likely that the higher dosage caused the overlapping, overcrowding, and blocking of UV irradiation, thereby reducing the availability of surface area for photocatalysis. For this reason, 80 g of the Sr-TiO_2/PCFM dosage was chosen for further experiments.

Effect of Initial HA Concentration

To assess the photocatalytic efficiency of initial concentrations, the photocatalytic experiment was carried out with the initial concentrations of HA in the range 15-65 mg/L. The equilibrium concentration of TOC after reaching an adsorption-desorption equilibrium was 13.8, 27.8, 42.4, and 60.1 mg/L for 15, 30, 45, and 65 mg/L of initial HA concentration, respectively.

In our study, the kinetics of HA degradation by Sr-TiO_2/PCFM were analyzed by using pseudo first-order kinetics, which is expressed by Eq. (22):

$$\ln\left(\frac{[TOC]_0}{[TOC]_t}\right) = kt \tag{22}$$

…where k is the pseudo first-order reaction rate constant (h^{-1}), $[TOC]_0$ and $[TOC]_t$ are the equilibrium concentrations of TOC after adsorption in the dark, and the remaining concentration of TOC at irradiation time t, respectively.

Fig. 7 shows the linear dependence of $ln([TOC]_0/[TOC]_t)$ on time t, while Table 5 presents the reaction rates and half-lives of decomposition of HA at various concentrations. All the curves showed good linear correlation (R^2>0.990), suggesting that the degradation of HA by Sr-TiO_2/PCFM followed the pseudo first-order kinetics. It was observed that the change of the initial HA concentration resulted in the change of the exposure time required to obtain complete degradation. The rate constants k of TOC removal decreased and the half-lives increased with increasing initial HA concentration in the solution. It has been asserted that when the HA concentration increased, more HA molecules covered or created the saturation on the photo-catalytically active surface of Sr-TiO_2/PCFM. Thus, a number of photons

Table 5. Degradation rate constants as the dependence of TOC concentration in photocatalytic oxidation of HA.

Concentration of HA (mg/L)	Reaction rate constant k (h^{-1})	Oxidation half-life (h)	Determination coefficient R^2
15	0.233	2.974	0.995
30	0.173	4.006	0.992
45	0.126	5.500	0.990
65	0.094	7.372	0.993

that interact with these sites decrease and deactivate the photocatalyst [26]. As a result, $OH^{\bullet}$ generation decreases and the degradation rate of HA also decreases. Moreover, it probably resulted from the complexity of the chemical structure and lower solubility in water of the HA compound undergoing mineralization to CO_2 and water together with byproduct formation. These results were consistent with several previous studies that have reported the dependency of the TiO_2 reaction rate on the concentration of contaminants in water [27]. A high concentration of pollutants in water saturates the catalyst surface and hence reduces the photonic efficiency and deactivation of the photocatalyst.

Effect of pH Values

Many reports about the effect of pH on photocatalytic degradation of organic compounds in water resource have been written [20, 28-29]. In fact, the interpretation of the pH-dependent photodegradation of HA on TiO_2 is a very difficult task because of its multiple roles.

The effect of pH on the removal of HA by using Sr-TiO_2/PCFM has been investigated. Four sets were conducted with the same initial HA concentration of 15 mg/L, but at different initial pH (3.98, 5.98, 6.96, and 9.80). Each of the sets was performed for 8 h. It was found that the pH values had a significant effect on the decomposition of HA in Fig. 8. The highest degradation was obtained in the acidic environment (pH = 3.98) next to the neutral ones, and the lowest was observed in the alkaline environment (pH = 9.80). The Sr-TiO_2/PCFM showed its higher photocatalytic activity under acidic conditions, which suggests that a certain group of HA compounds, such as carboxylic acids, was readily adsorbed onto the Sr-TiO_2/PCFM surface, confirming the finding of Bekbolet et al. [30] that TiO_2 has a strong affinity for HA, especially at low pH. Moreover, it was because the positively charged catalyst surface is conducive to the transferring process of photogenerated electrons to the surface of the catalyst, which contributes to the generation of active radicals such as $O_2^{\bullet-}$ and $OH^{\bullet}$, meanwhile avoiding the recombination of photogenerated electrons and holes. There was a sharp reduction of HA concentration at pH 3.98 during the first hour of photoreaction. This can be expressed as in the acidic environment, catalyst particles possess a positive charge and strongly attract anionic forms of HA. In contrast, at neutral pH (pH = 6.98) the catalyst surface is charged less, and catalyst particles are willing to form complexes. At high pH values the adsorption played a significant role in photocatalytic degradation. Lower photocatalytic degradation of HA at higher pH as the photoreaction mainly occurred on the surface of the catalyst, while HA could not adsorb onto the negatively charged Sr-TiO_2/PCFM surface. In addition, the carboxyl groups on the HA were ionized in an alkaline environment. A majority of phenolic groups will only be ionized above pH 9. This ionization led to a negative charge on the HA molecules, which led to a repulsion from the increasingly more negative TiO_2. Hence, the lowered adsorption led to a reduced rate as observed. This is in agreement with the results reported by Xue et al. [7] which evaluated the photocatalytic degradation of HA over TiO_2 particles on granular-activated carbon.

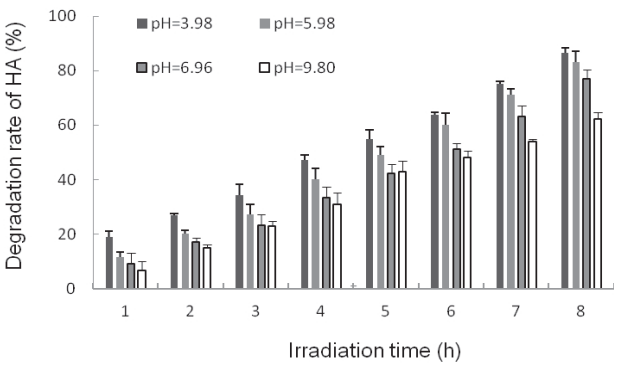

Fig. 8. Influence of pH on degradation of HA.

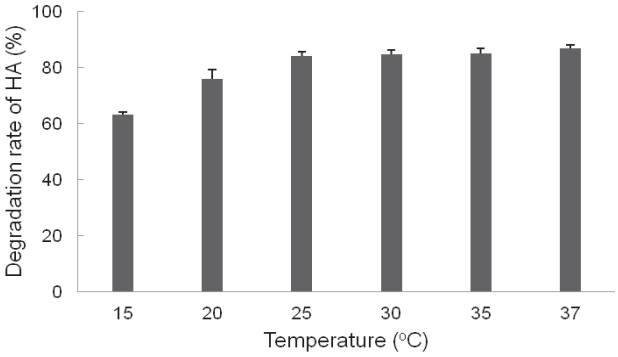

Fig. 9. Influence of temperature on degradation of HA.

Effect of Temperature

In fact, photocatalytic systems in most cases are operated at room temperature and do not require heating. At room temperature, the low thermal energy (0.026 eV) is inadequate to activate the TiO_2 surface, but it is quite close to the activation energy of hydroxyl radical formation. Thus, it can be assumed that the photodegradation rate of HA is governed by hydroxyl radical reactions, and the effect of temperature on the rate of oxidation may be dominated by the rate of interfacial electron transfer to oxygen [31].

In our experiments, temperatures were selected to simulate operating conditions during winter (15ºC) and summer (37ºC) in Wuhan, China. The effect of temperature on the photocatalytic degradation of HA onto Sr-TiO_2/PCFM was carried out at the same pH values and initial HA concentration of 15 mg/L.

The degradation of HA in the water resource at different temperatures is presented in Fig. 9, which shows that the higher operating temperatures slightly enhance degradation at the same pH under UV irradiation. In other words, the degradation of HA fluctuated with

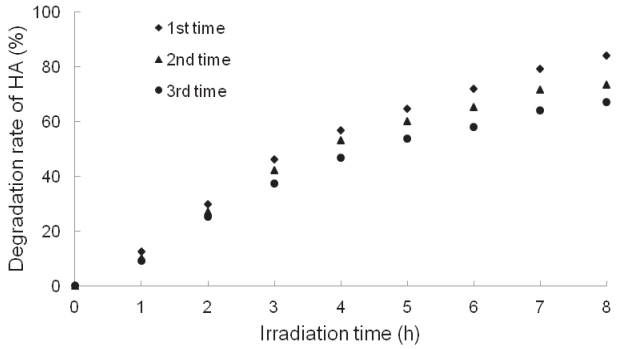

Fig. 10. Degradation rate of HA by repeated use of Sr-TiO_2/PCFM (initial HA concentration = 15 mg/L, irradiation time = 8 h, temperature = 25 ±2ºC).

increasing temperature, which was consistent with that reported by Palmer et al. [32]. These results were not surprising because of temperature, which for instance can increase the interfacial charge transfer rate and the rate of indirect oxidation in homogeneous solution by changing the number of charge carriers and the rate constant. Alternatively, a contributory factor to this effect is probably the more rapid desorption of both substrate and intermediates from the catalyst particles, giving a larger effective surface area.

Photocatalytic Stability of Sr-TiO_2/PCFM

One of the most important factors in water treatment is the reuse of a photocatalyst for its practical application. Sr-TiO_2/PCFM was reused several times for the HA degradation to evaluate its photocatalytic stability. As shown in Fig. 10, more than 84% HA was degraded at the first cycle. The removal of HA was slightly reduced as reuse times increase. After 3 cycles, the removal efficiency of HA was above 67.3% of the initial concentration after photocatalytic reaction of 8 h. Additionally, TiO_2 supported on PCFM did not leach into the water resource during the reuse process. These results indicate that Sr-TiO_2/PCFM is a very stable photocatalyst for photocatalytic degradation of HA. Thus, reusability is a significant advantage of Sr-TiO_2/PCFM to reduce cost and factors harmful to the environment.

Conclusions

In conclusion, the strontium-doped TiO_2 coated on porous ceramic filter media (Sr-TiO_2/PCFM) was successfully prepared through the heating process. Adsorption characteristics and photocatalytic activity of Sr-TiO_2/PCFM were evaluated by the removal of HA from the water resource. We discovered that the adsorption equilibrium of HA was reached in about 4 h for 15 mg/L of initial HA concentration with 80 g of Sr-TiO_2/PCFM employed. The adsorption of HA on Sr-TiO_2/PCFM followed both Langmuir and Freundlich models and fitted the pseudo second-order kinetics model. The degradation efficiency of HA by Sr-TiO_2/PCFM followed the pseudo first-order kinetics and depended on Sr-TiO_2/PCFM dosage, initial HA concentration, pH, and temperature. The Sr-TiO_2/PCFM is reusable with good photocatalytic activity after three cycles. Further research to investigate the degradation of HA from real surface water is required in order to better comprehend the Sr-TiO_2/PCFM applications.

Acknowledgments

This work was supported by the Major Science and Technology Program for Water Pollution Control and Treatment of China's 12th Five-Year Plan (No. 2012ZX07101007-005), the Hubei Provincial Natural Science Foundation of China (No. 2014CFB282), and the Knowledge Innovation Program of the Chinese Academy of Sciences. The authors would like to thank all of their teachers as well as other laboratory colleagues in the School of Resources and Environmental Engineering, Wuhan University of Technology and in the laboratory of the Institute of Hydrobiology, Chinese Academy of Science for assistance during the work. Additionally, we appreciate the constructive suggestions of the anonymous reviewers, which proved to be invaluable for improving the quality of the manuscript.

References

1. HASSAN K., BIJIAN B., JAVAD K. Evaluation of UV/TiO_2 photo-catalytic process for removing humic compounds from water. Polish journal of environmental studies **24** (3), 1063, **2015**.
2. BEAK M.H., YOON J.W, HONG J.S, SUH J.K. Application of TiO_2 - containing mesoporous spherical activated carbon in a fluidized bed photoreactor - Adsorption and photocatalytic activity. Applied Catalysis A: General **450**, 222, **2013**.
3. SHENG G., YANG Q., PENG F., LI H., GAO X., HUANG Y. Determination of colloidal pyrolusite, Eu (III) and humic substance interaction: a combined batch and EXAFS approach. Chemical Engineering Journal **245**, 10, **2014**.
4. ZAWISZA B., BARANIK A., MALICKA E., TALIK E., SITKO R. Preconcentration of Fe(III), Co(II), Ni(II), Cu(II), Zn(II) and Pb(II) with ethylenediamine-modified graphene oxide. Microchimica Acta. **183**, 231, **2016**.
5. YANG S., HU J., CHEN C., SHAO D. WANG X. Mutual effects of Pb(II) and humic acid adsorption on multiwalled carbon nanotubes/polyacrylamide composites from aqueous solutions. Environ. Sci. Technol. **45** (8), 3621, **2011**.
6. WANG W., LI H., DING Z., WANG X. Effects of advanced oxidation pretreatment on residual aluminum control in high humic acid water purification. Journal of Environmental Sciences **23** (7), 1079, **2011**.
7. XUE G., LIU H., CHEN Q., HILLS C., TYRER M., INNOCENT F. Synergy between surface adsorption and photocatalysis during degradation of humic acid on TiO_2/activated carbon composites. Journal of Hazardous Materials **186** (1), 765, **2011**.

8. WANG P.F, QI N., AO Y.H., HOU J., WANG C., QIAN J. Effect of UV irradiation on the aggregation of TiO_2 in an aquatic environment: Influence of humic acid and pH. Environmental Pollution **212**, 178, **2016**.
9. ANDAYANI W., BAGYO A.N.M. TiO_2 beads for photocatalytic degradation of humic acid in peat water. Indo. J. Chem. **11** (3), 253, **2011**.
10. MIODUSKA J., ZIELINSKA-JUKER A., HUPKA J. Photocatalytical degradation of toluene and cyclohexane using LED illumination. Polish journal of environmental studies **26** (3), 1159, **2017**.
11. JEON J.H., KIM S.D., LIM T.H., LEE D.H. Degradation of trichloroethylene by photocatalysis in an internally circulating slurry bubble column reactor. Chemosphere **60** (8), 1162, **2005**.
12. QUINLIVAN P.A., LI L., KNAPPE D.R.U. Effects of activated carbon characteristics on the simultaneous adsorption of aqueous organic micro-pollutants and natural organic matter. Water Res. **39** (8), 1663, **2005**.
13. ZHANG Y., HE F., XIA S.B, KONG L.W, XU D., WU Z.B. Adsorption of sediment phosphorus by porous ceramic filter media coated with nano-titanium dioxide film. Ecological Engineering **64**, 186, **2014**.
14. WANG X, LIU Y.F., HU Z.H, CHEN Y.J., LIU W., ZHAO G.H. Degradation of methyl orange by composite photocatalysts nano-TiO_2 immobilized on activated carbons of different porosities. Journal of Hazardous Materials **169** (1-3), 1061, **2009**.
15. DOGAN M., ALKAN M., DEMIRBAS Ö., ÖZDEMIR Y., ÖZMETIN C. Adsorption kinetics of maxilon blu GRL onto sepiolite from aqueous solution. Chem. Eng. J. **124**, 89, **2006**.
16. BEAK M.H., IJAGBEMI C.O., O S.J., KIM D.S. Removal of Malachite Green from aqueous solution using degreased coffee bean. Journal of Hazardous Materials **176** (1-3), 820, **2010**.
17. WEI D., LI M.T., WANG X.D., HAN F., LI L.SH, GUO J., AI L.J., FANG L.L., LIU L., DU B., WEI Q. Extracellular polymeric substances for Zn (II) binding during its sorption process onto aerobic granular sludge. Journal of Hazardous Materials **301**, 407, **2016**.
18. MAGHSOODLOO SH., NOROOZI B., HAGHI A.K., SORIAL G.A. Consequence of chitosan treating on the adsorption of humic acid by granular activated carbon. Journal of Hazardous Materials **191** (1-3), 380, **2011**.
19. LAZAR M., VARGHESE S., NAIR S. Photocatalytic water treatment by titanium dioxide: Recent updates. Catalysts **2** (4), 572, **2012**.
20. CHONG M.N., JIN B., CHOW C.W.K., SAINT C. Recent developments in photocatalytic water treatment technology: A review. Water research **44** (10), 2997, **2010**.
21. SUN Q., LI H., NIU B.J., HU X.L., XU C.H., ZHENG S.L. Nano-TiO_2 immobilized on diatomite: characterization and photocatalytic reactivity for Cu^{2+} removal from aqueous solution. Procedia Engineering **102**, 1935, **2015**.
22. NISHANTHI S.T., IYYAPUSHPAM S., SUNDARAKANNAN B., SUBRAMANIAN E., PADIYAN D.P. Significance of crystallinity on the photoelectrochemical and photocatalytic activity of TiO_2 nanotube arrays. Applied Surface Science **313**, 449, **2014**.
23. WANG H.T., YE Y.Y., QI J., LI F.T., TANG Y.L. Removal of titanium dioxide nanoparticles by coagulation: effects of coagulants, typical ions, alkalinity and natural organic matters. Water Sci. Technol. **68** (5), 1137, **2013**.
24. YI Z., FENG H., ENRONG X., YIMIN Z., SHIBIN X., ZHENBIN W. Photocatalytic reduction of phosphorus in the acid pickling milling wastewater from high-phosphorus hematite mineral processing. Desalination and Water Treatment **40** (1-3), 38, **2012**.
25. XIAO Y.T., XU S.S., LI Z.H, AN X.H., ZHOU L., ZHANG Y.L., SHIANG F.Q. Progress of applied research on TiO_2 photocatalysis-membrane separation coupling technology in water and wastewater treatments. Chinese Science Bulletin **55** (14), 1345, **2010**.
26. GAYA U.I., ABDULLAH A.H. Heterogeneous photocatalytic degradation of organic contaminants over titanium dioxide: A review of fundamentals, progress and problems. Journal of Photochemistry and Photobiology C: Photochemistry Reviews **9** (1), 1, **2008**.
27. CHONG M.N., LEI S., JIN B., SAINT C., CHOW C.W.K. Optimisation of an annular photoreactor process for degradation of Congo Red using a newly synthesized titaniaim pregnated kaolinite nano-photocatalyst. Separation and Purification Technology **67** (3), 355, **2009**.
28. MOZIA S. Photocatalytic membrane reactors (PMRs) in water and wastewater treatment. A review. Separation and Purification Technology **73** (2), 71, **2010**.
29. UMAR M., ABDUL H.A. Photocatalytic Degradation of Organic Pollutants in Water, in: Rashed, M. N., (Eds.), Organic Pollutants - Monitoring, Risk and Treatment, Publisher: InTech, 195, **2013** http://dx.doi.org/10.5772/53699.
30. BEKBOLET M., SUPHANDAG A.S., UYGUNER C.S. An investigation of the photocatalytic efficiencies of TiO_2 powders on the decolourisation of humic acids. Journal of Photochemistry and Photobiology A: Chemistry. **148** (1-3), 121, **2002**.
31. MILLS A., HUNTE S. L. An overview of semiconductor photocatalysis. Journal of Photochemistry and Photobiology A: Chemistry **108** (1), 1, **1997**.
32. PALMER F.L., EGGINS B.R., COLEMAN H.M. The effect of operational parameters on the photocatalytic degradation of humic acid. Journal of Photochemistry and Photobiology A: Chemistry **148** (1-3), 137, **2002**.